Indium plasma in single- and two-color mid-infrared fields: Enhancement of tunable harmonics

R. A. Ganeev,[1,2,*] Zhe Wang,[3] Pengfei Lan,[4] Peixiang Lu,[3,4] M. Suzuki,[1] and H. Kuroda[1]

[1]*Ophthalmology and Advanced Laser Medical Center, Saitama Medical University, 38 Morohongo, Moroyama-machi, Iruma-gun, Saitama 350-0495, Japan*

[2]*Faculty of Physics, Voronezh State University, Voronezh 394006, Russia*

[3]*Laboratory of Optical Information Technology, Wuhan Institute of Technology, Wuhan 430205, China*

[4]*Wuhan National Laboratory for Optoelectronics and School of Physics, Huazhong University of Science and Technology, Wuhan 430074, China*

(Received 1 December 2015; published 26 April 2016)

The tuning of odd and even high-order harmonics of ultrashort pulses along the strong resonance of laser-produced indium plasma using an optical parametric amplifier of white-light continuum radiation (1250–1400 nm) allowed observation of different harmonics enhanced in the vicinity of the $4d^{10}5s^2\,{}^1S_0 \rightarrow 4d^9 5s^2 5p\,{}^1P_1$ transition of In II ions. We demonstrate various peculiarities and discuss the theoretical model of the phenomenon of tunable harmonics enhancement in the region of 62 nm using indium plasma. With the theoretical analysis we can reproduce the experimental observations and characterize the dynamics of the resonant harmonic emissions.

DOI: 10.1103/PhysRevA.93.043848

I. INTRODUCTION

The search for new methods for materials science using optical and nonlinear optical approaches is an important goal of laser physics. High-order-harmonic generation (HHG) of laser radiation has long been considered a promising spectroscopic tool to retrieve the structural and dynamical information regarding a nonlinear medium through analysis of the spectra, polarization states, and phase of generated harmonics [1–3]. Photorecombination, the third step in the HHG recollision model [4,5], is the inverse process of photoionization [6] and therefore it is expected that HHG and photoionization must exhibit common resonances in the case of both laser-produced plasmas (LPPs) [7,8] and gases [9].

The resonance peaks in the photoionization and photorecombination cross sections, including autoionizing [10], shape [11], and giant resonances [12], have long been investigated. In contrast, studies on the role of resonances in HHG are relatively scarce. Forming resonance conditions to enhance the nonlinear optical response of the medium may be an alternative to the phase-matching technique previously used for harmonic enhancement. The role of atomic resonances in increasing the laser radiation conversion efficiency was actively discussed in the framework of perturbation theory at the early stages of the study of low-order harmonic generation [13]. Resonance enhancement introduces an additional possibility of increasing the conversion efficiency of a specific harmonic order by more than one order of magnitude. If this effect could be combined with phase-matching effects and/or coherent control of HHG, one might be able to generate a spectrally pure coherent x-ray source with only a single line in the spectrum, much like saturated x-ray lasers produced by ionic population inversions in highly ionized plasmas.

The effects of approximately fixed pump laser wavelength in resonant harmonics were reported a long time ago [14] using Ti:sapphire lasers. In those studies, fine tuning was accomplished either by using a chirping technique within the pulse bandwidth or by insignificant variation of the master oscillator wavelength. In the present studies the tuning of the pump laser wavelength was dramatically improved compared with the above-mentioned case, which allowed changing of the intensity ratios of various harmonics particularly near 62 nm in the case of the HHG in the indium plasma, thus forming the conditions for resonance enhancement of different orders of harmonics near resonances possessing large oscillator strength. Various theoretical approaches for description of resonant HHG were introduced in Refs. [15–24]. For these approaches it is important that the harmonic wavelength is resonant with the transition between the ground state and the autoionizing state (AIS) of the generating ion and that this transition possesses strong oscillator strength. Particularly in the so-called four-step model [21] the ionized and laser-accelerated electron is captured into the AIS (i.e., an excited state embedded in the continuum) of the parent ion, and, in the final step, during the radiative relaxation of this state to the ground state, a harmonic photon is emitted.

The unavailability of tuning of the wavelength of the most frequently used Ti:sapphire lasers significantly restricts the probability of coincidence of the harmonic order and the transition between AIS and ground states possessing a large value of the oscillator strength. To facilitate the use of the plasma harmonic concept for laser-ablation-induced HHG spectroscopy in the extreme ultraviolet (XUV) range, one should use tunable sources of laser radiation allowing the fine tuning of driving pulses and correspondingly harmonic wavelengths along the spectral ranges of strong ionic transitions.

In general, the question arises as to why similar resonant harmonics have not been observed with gas media. Tunable femtosecond lasers are now available, and so there should be no problem tuning the laser wavelength to a specific resonance, whether it be of a plasma or a gas. The answer to this question is related to the basic principles of the role of resonances in the enhancement of nearby harmonics. In most cases the harmonic spectra show the absence of enhancement of the harmonics

*rashid_ganeev@mail.ru

near strong emission lines. In the meantime, previous studies have demonstrated that the resonance enhancement of nearby harmonics close to the resonance can be observed in the case of a sufficient amount of excited species (i.e., singly or doubly charged ions). Thus the availability of resonance enhancement depends on the population of the appropriate energetic levels of ions.

The studies of high-order nonlinear processes through exploitation of intermediate resonances show that the proximity of the wavelengths of specific harmonic orders and the strong emission lines of ions does not necessarily lead to the growth of the yield of a single harmonic. The nonlinear optical response of the medium during propagation of intense pulses includes, in some particular cases, the resonance-induced enhancement of specific nonlinear optical processes, the absorption of emitted radiation, and the involvement of collective macroprocesses, such as phase matching between the interacting waves. The mechanism for improvement of the phase-matching conditions for a single harmonic can be interpreted in that case as follows. The refractive index of plasma in the short-wavelength side of some resonant transitions can be decreased due to anomalous dispersion, thus allowing the coincidence of the refractive indices of plasma at the wavelengths of the driving and harmonic waves. To analyze this process in depth one has to define the bandwidths of those resonances, the relative role of the nonlinear enhancement of harmonic emission and the absorption properties of a LPP in the vicinity of resonances, the influence of the plasma length on the enhancement of a single harmonic, etc.

In this paper, we demonstrate the fine tuning of harmonics in the vicinity of the strong In II transition during HHG using a mixture of a tunable mid-infrared (MIR) source of ultrashort pulses and its second harmonic (H2) in the LPP produced on the surface of an indium target, analyze the enhancement of those harmonics, and compare them with a single-color MIR pump. We also present a theoretical description of the observed phenomena.

II. EXPERIMENTAL ARRANGEMENTS FOR HHG IN INDIUM PLASMA USING TUNABLE MIR PULSES

The experimental setup consisted of a Ti:sapphire laser, a traveling-wave optical parametric amplifier (OPA) of the white-light continuum, and a HHG scheme using propagation of the amplified signal pulses from the OPA through the extended LPP [Fig. 1(a)]. We used a mode-locked Ti:sapphire laser (Tsunami, Spectra-Physics Lasers) pumped by a diode-pumped, cw laser (Millenia Vs, SpectraPhysics Lasers) as the source of 803 nm, 55 fs, 82 MHz, 450 mW pulses for injection in the pulsed Ti:sapphire regenerative amplifier with pulse stretcher and additional double-passed linear amplifier (TSA-10, Spectra-Physics Lasers). The output characteristics from this laser were as follows: central wavelength 810 nm, pulse duration 350 ps, pulse energy 5 mJ, 10 Hz pulse repetition rate. This radiation was further amplified up to 22 mJ in the home-made three-pass Ti:sapphire linear amplifier. Part of the amplified radiation with pulse energy of 6 mJ was separated from the whole beam and used as a heating pulse for homogeneous extended plasma formation using a 200 mm focal length cylindrical lens installed in front of the extended

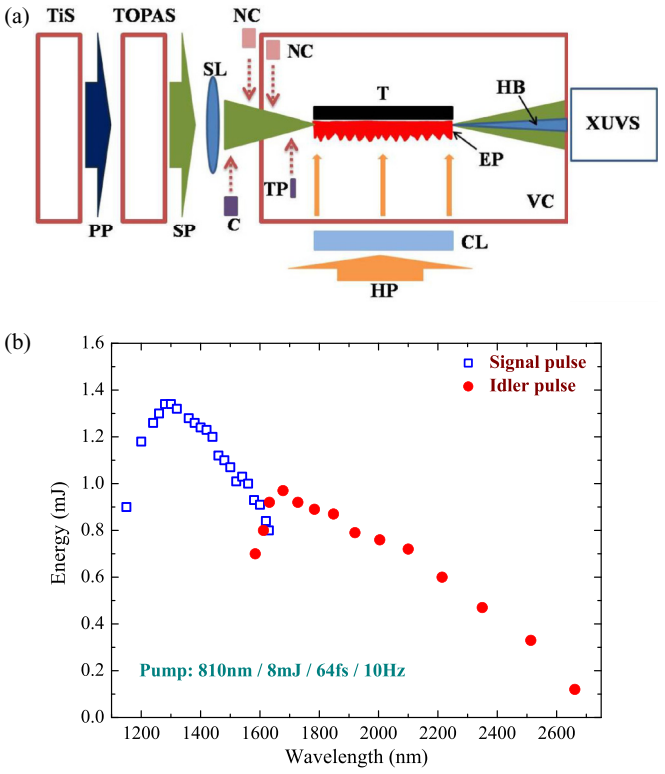

FIG. 1. (a) Experimental setup. TiS, Ti:sapphire laser; TOPAS, optical parametric amplifier; PP, pump pulse for pumping the optical parametric amplifier; SP, amplified signal pulse from OPA; HP, heating picosecond pulse from Ti:sapphire laser; SL, spherical lens; CL, cylindrical lens; VC, vacuum chamber; T, target; EP, extended indium plasma; NC, nonlinear crystal (BBO); C, calcite; TP, thin glass plates; HB, harmonic beam; XUVS, extreme ultraviolet spectrometer. (b) Spectral tuning of mid-infrared signal and idler pulses.

indium target placed in the vacuum chamber. We analyzed the indium plasma as the medium for harmonic generation using a tunable source of ultrashort pulses. The 5-mm-long sample of bulk indium was installed in the vacuum chamber for laser ablation. The intensity of the heating pulse on the target surface was varied up to 4×10^9 W cm^{-2}. The ablation sizes were 5×0.08 mm^2.

The remaining part of the amplified radiation was delayed with regard to the heating pulse. After compression and pumping of the OPA, the signal or idler pulse from the parametric amplifier propagated through the LPP for 35 ns from the beginning of target irradiation by the heating pulses. After propagation of the compressor stage the output characteristics of the Ti:sapphire laser were as follows: pulse energy 8 mJ, pulse duration 64 fs, 10 Hz pulse repetition rate, pulse bandwidth 17 nm, central wavelength 810 nm. This radiation pumped the OPA (He-Topas Prime, Light Conversion). The signal and idler pulses from the OPA allowed tuning along the 1200–1600 nm and 1600–2600 nm ranges, respectively [Fig. 1(b)].

In our HHG experiments we used the signal pulses, which were 1.5 times stronger than the idler pulses. These experiments were carried out using 1 mJ, 70 fs pulses tunable in the range of 1250–1400 nm. This variation of the driving

pulse wavelength was sufficient for tuning the harmonics along various resonances of ionic species. The spectral bandwidth of the tunable pulses was 45 nm. The intensity of the 1310 nm pulses focused by a 400-mm-focal-length lens through the 3-mm-thick MgF_2 window of the vacuum chamber into the extended plasma was 2×10^{14} W cm^{-2}. These driving pulses were focused at a distance of $\sim$150 μm above the target surface. The plasma and harmonic emissions were analyzed using an XUV spectrometer containing a cylindrical mirror and a 1200 grooves/mm flat field grating with variable line spacing. The spectrum was recorded on a microchannel plate detector with a phosphor screen, which was imaged onto a CCD camera.

Our experiments were carried out using both the single-color and two-color pumps of the LPP. The reasons for using the double-beam configuration to pump the extended plasma is related to the small energy of the driving MIR signal pulse ($\sim$1 mJ). The $I_H \propto \lambda^{-5}$ rule (I_H is the harmonic intensity and λ is the driving field wavelength [25]) led to a significant decrease of harmonic yield in the case of longer-wavelength sources compared with the 810 nm pump and did not allow the observation of strong harmonics from the single-color MIR (1310 nm) pulses. Because of this we used the second-harmonic (H2) generation of the signal pulse to apply the two-color pump scheme (MIR + H2) for plasma HHG. A 0.5-mm-thick beta barium borate (β-BaB_2O_4, BBO) crystal was installed inside the vacuum chamber on the path of focused signal pulse [Fig. 1(a)]. The BBO was cut at $\theta = 21^\circ$ and adjusted to the phase matching for a 1310 nm wavelength. At these conditions, it was not necessary to tune the crystal for each OPA wavelength due to the small dispersion in the 1240–1400 nm range. The conversion efficiency of 655 nm pulses was $\sim$27%. The spectral bandwidth of the second-harmonic pulse was 22 nm. The two orthogonally polarized pump pulses were sufficiently overlapped both temporally and spatially in the extended plasma, which led to a significant enhancement of odd harmonics, as well as generation of even harmonics of similar intensity as the odd ones.

The variation of the relative phase between fundamental and second-harmonic waves was analyzed by insertion of 0.15-mm-thick glass plates in the path of these beams. The plates were introduced between the BBO crystal and the LPP, as shown in Fig. 1(a). The group-velocity dispersion for the driving and second-harmonic waves propagating through such plates makes possible the variation of both the relative phase of the two pumps and the delay between the envelopes of these pulses.

We also analyzed the conditions for the two-color pump of the plasma using different polarizations of interacting waves when the BBO crystal was installed outside the vacuum chamber. We inserted a2-mm-thick calcite plate in front of the BBO crystal at the conditions when the MIR pulses generate H2 in a 0.7-mm-thick BBO crystal placed between the focusing lens and the input window of the vacuum chamber. The rotation of the calcite affected only the driving pulse by changing the polarization from linear to elliptical and to circular. In that case the two-color pump consisted of the linearly polarized second-harmonic wave and circularly (or elliptically) polarized fundamental MIR pulses.

III. EXPERIMENTAL STUDIES OF THE RESONANCE ENHANCEMENT OF MIR-INDUCED HARMONICS IN INDIUM PLASMA

The harmonics generated in indium plasma using MIR pulses (1 mJ, 1330 nm) were significantly weaker compared with the case of the 8 mJ, 810 nm pump due to the above-mentioned wavelength-dependent yield of the harmonics. The comparison of these two pumps at similar energies of pulses (1 mJ) showed a sevenfold decrease of the harmonic yield in the plateau region using 1330 nm pulses compared with the 810 nm pulses [Fig. 2(a)], while the theoretical prediction of this ratio was $I_{1330\,\mathrm{nm}}/I_{810\,\mathrm{nm}} = (810\,\mathrm{nm}/1330\,\mathrm{nm})^{-5} \approx 12$. The observed harmonic cutoff in the case of MIR pulses was approximately similar to the one from the 810 nm pump [27 eV (H29) and 26 eV (H17), respectively], contrary to the theoretically expected extension of the cutoff energy for the longer-wavelength pump ($E_{\mathrm{cutoff}} \propto \lambda^2$), due to the very small conversion efficiency in the case of MIR pulses, which did not allow the observation of harmonics below the 40 nm spectral region. We also used the weak idler pulses from the OPA, with the energy varying in the range of 0.3–0.5 mJ, for harmonic generation in plasma. Even these small energies of driving longer-wavelength pulses were sufficient to observe the resonance enhancement of different harmonic orders near the AIS of indium in the case of idler pulses tunable along the 1730–2100 nm range [Fig. 2(b)].

These studies showed that the use of tunable MIR pulses caused generation of mostly a single enhanced harmonic (H21) close to the AIS and a few weak odd harmonics in the longer-wavelength range of XUV radiation [Fig. 3(a)]. The insertion of the BBO crystal into the path of the focused driving beam drastically modified the harmonic spectra. Extension of the observed harmonic cutoff, significant growth of the yield of odd harmonics, comparable harmonic intensities for the odd and even orders along the whole range of generation, tuning of harmonics allowing the optimization of resonance-induced single-harmonic generation, as well as a few neighboring orders close to the AIS of indium, were among the advanced features of these two-color experiments [Fig. 3(b)]. These studies showed that the advantage of the resonance-induced enhancement of harmonics using MIR + H2 pulses is an opportunity for fine tuning of this high-order nonlinear optical process for spectral enhancement of the harmonic yield. Another advantage is closely related with the analysis of the oscillator strengths of some ionic transitions using the HHG approach.

Various schemes for the two-color pump for HHG were introduced in Refs. [26–33]. As underlined in [33], a strong harmonic generation in the case of a two-color pump is possible due to formation of a quasilinear field, selection of a short quantum path component, which has a denser electron wave packet, and higher ionization rate compared with the single-color pump. The orthogonally polarized second field also participates in the modification of the trajectory of the accelerated electron from being two dimensional to three dimensional, which may lead to removal of the medium's symmetry. With suitable control of the relative phase between the fundamental and second-harmonic pumps, the latter field enhances the short-path contribution while diminishing other electron paths, resulting in a clean spectrum of harmonics.

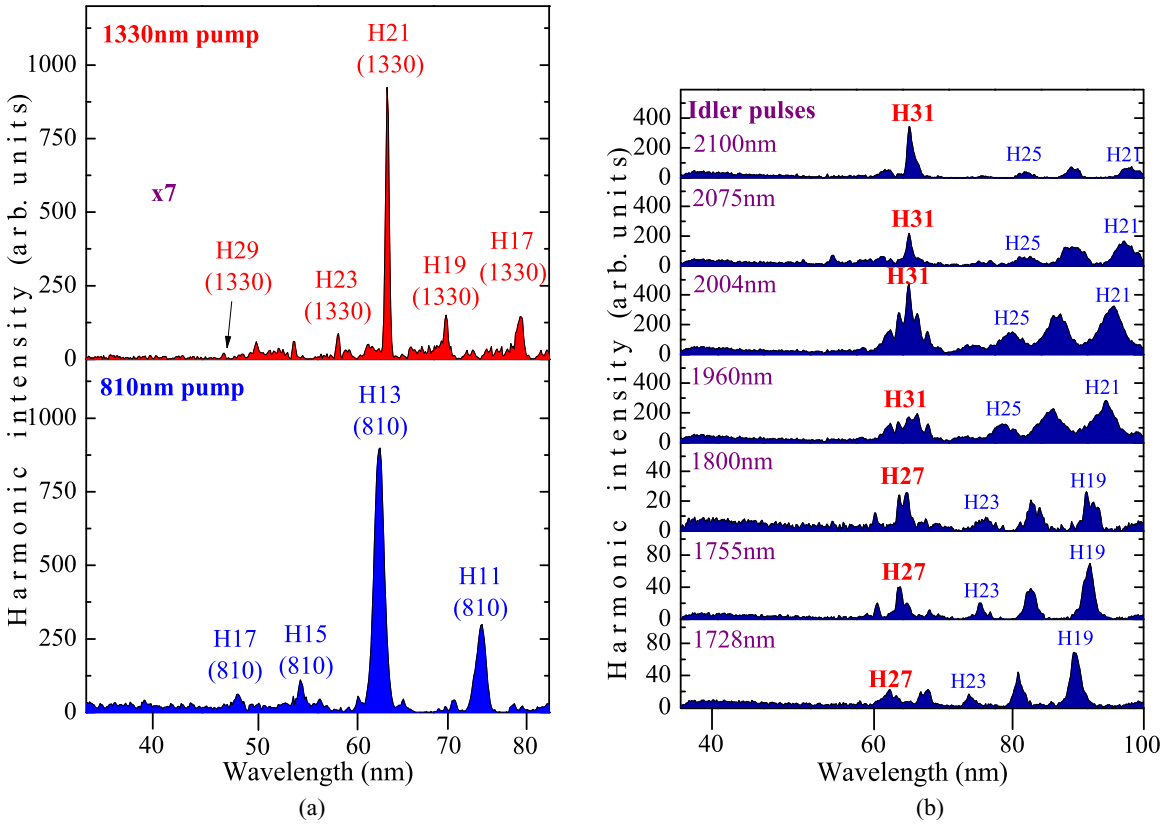

FIG. 2. (a) Harmonic spectra using 1330 nm (upper panel) and 810 nm (lower panel) pulses. Upper panel magnified by a factor of 7 for better comparison of the harmonic spectra generated using different pumps. (b) Spectra of tunable harmonics in the case of single-color pump of indium plasma using idler (1728–2100 nm) pulses of OPA.

The use of tunable broadband MIR radiation and its second harmonic allowed the analysis of the enhancement of the groups of harmonics close to the resonance possessing strong oscillator strength [Fig. 3(c)]. One can see the growth of harmonic yield in the 62.3 nm region of the AIS for different groups of harmonics during tuning of the wavelength of the driving pulses. These studies using tunable MIR pulses and their second harmonics showed a fine tuning of the resonance-enhanced harmonic and change of the order of this harmonic. The tunability is practically unlimited since the tuning of the fundamental wavelength [Fig. 1(b)] allowed shifting the wavelength of the high-order harmonic over the wavelength of the neighboring harmonic, which means the overlap of a full octave.

The two upper panels of Fig. 4(a) show the harmonic spectra in the case of using two different schemes when the BBO crystal was installed either inside or outside the vacuum chamber. In the latter case, the linearly polarized 1330 nm pulses generated H2 in the 0.7-mm-thick BBO placed outside the vacuum chamber. In the case shown in the bottom panel of Fig. 4(a), the polarization of the driving 1330 nm pulses was changed from linear to circular by inserting the calcite plate in front of the BBO crystal. In that case the pump radiation after propagation of the BBO crystal consisted of a circularly polarized 1330 nm pump and a linearly polarized 665 nm pump. This apparently led to generation of high-order harmonics only from the 665 nm pump, which is seen in the bottom graph of this figure, showing the odd harmonics of H2 radiation.

In the two-color pump HHG experiments in gases, the variation of the relative phase between fundamental and second-harmonic waves of 30 fs pulses allowed observation of the threefold beatings between the long- and short-trajectory-induced harmonics [34]. The use of the focusing optics inside the XUV spectrometer in our experiments did not allow distinguishing the influence of the short and long trajectories of accelerated electrons on the divergence of harmonics. However, we observed the difference in the plasma harmonic spectra when thin (0.15 mm) glass plates were introduced between the BBO crystal and the plasma [Fig. 1(a)]. Examples of both decrease of the two-color field in the plasma area and decrease of the resonance enhancement of H21 are presented in Fig. 4(b). Thin glass plates were inserted after the BBO crystal to analyze the variation of the relative phase between the two pumps and to compare the change of relative intensities of "resonant" (H21) and "nonresonant" (H13) harmonic yields. One can see a significant departure from the large ratio H21:H13 in the case of the absence of the glass plates, which are actually relative phase modulators [upper panel of Fig. 4(b)], towards the low ratio of these harmonics in the case of propagation through six 0.15-mm-thick plates (bottom panel). Thus the variation of relative phase between pumps may diminish the role of the AIS in the single-harmonic enhancement. The decrease of pump intensity (due to the growth of Fresnel losses during reflection from a few plates) may also cause a decrease of the overall nonlinear response.

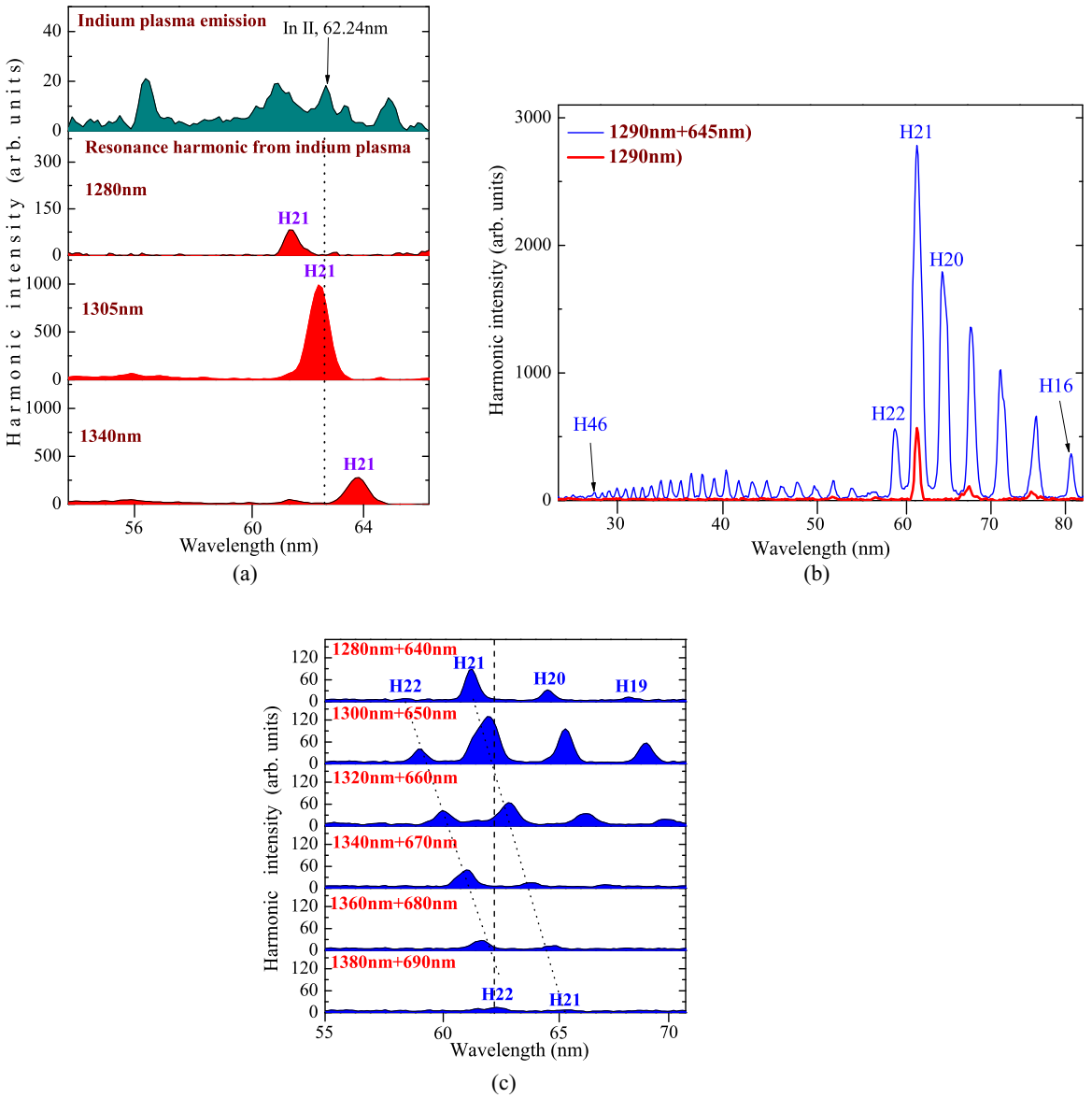

FIG. 3. (a) Tuning of H21 along the In II resonance. Upper panel shows the indium plasma emission spectrum. Three bottom panels show resonantly enhanced harmonic using single-color pump (1280, 1305, and 1340 nm, respectively). Dotted line shows the position of the resonance transition of In II. (b) Comparative harmonic spectra from indium plasma using single-color (1290 nm; thick curve) and two-color (1290 nm and 645 nm; thin curve) pumps. (c) Relative variations of H21 and H22 yields using different wavelengths of MIR and H2 pump radiation. Dotted lines show the tuning of H21 and H22. Dashed line shows the position of the resonance transition.

The relation between the addition of a single 0.15-mm-thick borosilicate crown glass (BK7) plate and the relative phase shift between fundamental and second-harmonic waves depends on the group-velocity dispersion in the glass. The group-velocity dispersion leads to a change of the relative phase between waves, and, in the case of thick samples, may lead to the temporal walkoff of two pulses. In particular, due to this effect in BK7, the 650 nm pulse (2ω) was delayed in the 0.15-mm-thick glass by $\Delta_{\mathrm{BK7}} = d[(n^{\mathrm{o}}_{\omega})_{\mathrm{group}}/c - (n^{\mathrm{e}}_{2\omega})/c] \approx$ 1.3 fs with respect to the 1300 nm pulse (ω) because $n^{\mathrm{o}}_{\omega} < n^{\mathrm{e}}_{2\omega}$ in this positive optical element. Here Δ_{BK7} is the delay between two pulses after leaving the thin glass, d is the glass thickness, $c/(n^{\mathrm{o}}_{\omega})_{\mathrm{group}}$ and $c/(n^{\mathrm{e}}_{2\omega})_{\mathrm{group}}$ are the group velocities of the ω and 2ω waves in the BK7, c is the light velocity, and n^{o}_{ω} and $n^{\mathrm{e}}_{2\omega}$ are the refractive indices of BK7 at the wavelengths of the ω and 2ω pumps. In the case of MIR pulses, the group-velocity dispersion between fundamental and second-harmonic waves was notably smaller compared with the case of Ti:sapphire laser radiation. Here we also mention the delay between two pulses in the output of the BBO crystal. In the case of 0.5-mm-thick BBO, the calculated walkoff between 1300 and 650 nm waves was 24 fs. Note that $t_{2\omega}$ at the output of the 0.5-mm-long BBO crystal was estimated to be 76 fs, while the 1300 nm pulse duration was 70 fs. The additional plates of BK7 led to a change of the relative phase and some decrease of the delay between the envelopes of fundamental and second-harmonic waves. The relative phase ϕ is proportional to the delay between envelopes ΔT and the carrier frequency ν_0 ($\phi \approx 2\pi\,\Delta T\,\nu_0$) [35]. Thus the single BK7 plate provides $\sim 0.1\pi$ variation of the relative phase.

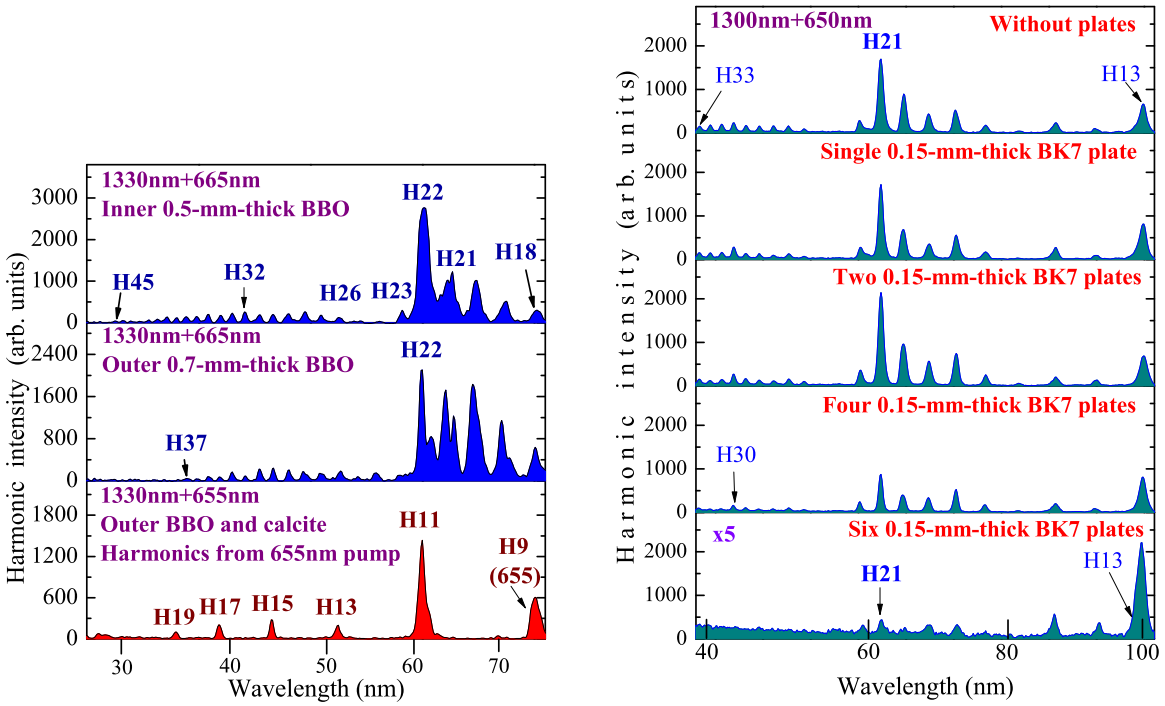

FIG. 4. (a) Harmonic spectra generated using the BBO crystal inserted inside (top panel) and outside (middle panel) the vacuum chamber. Bottom panel shows generation of the odd harmonics of 655 nm radiation once the calcite plate was installed in front of the BBO crystal, which led to variation of the polarization of the MIR pulse from linear to circular. (b) Harmonic spectra for variable phase difference between the MIR and H2 pulses. One can see a gradual change of the relative intensities of H13 and resonance-enhanced H21 using different numbers of inserted 0.15-mm-thick BK7 plates.

In our experiments, the HHG occurred in quite a long medium (5 mm). Below we discuss the role of the propagation effect in this kind of experiment. To achieve higher HHG conversion efficiency, the length of the medium might be increased provided that the phase mismatch between the laser field and the harmonic radiation remains low [36]. For medium lengths where the reabsorption can be neglected and for the optimum phase-matching conditions, the harmonic intensity increases as the square of the medium length. However, once the medium length exceeds the coherence length, the harmonic intensity shows oscillations due to phase mismatch [37]. To analyze this propagation process in the LPP, one has to carefully define the best conditions for plasma HHG in the extended medium, while taking into account the peculiar properties of the indium used for laser ablation.

Initially, we analyzed the dependence of the harmonic yield on the length of indium plasma and found the slope of this curve to be close to 2 in the appropriately ablated plasma until the maximum length used in these experiments (5 mm). The following studies were carried out at the conditions of this "optimal" LPP. Note that application of stronger ablation of the indium target led to decrease of the harmonic yield due to phase mismatch caused by the large amount of free electrons. In that case the coherent length of high-order harmonics became shorter than the length of homogeneous extended plasma. The above-mentioned dependence deviated from the slope of 2. To overcome this propagation effect one can use the quasi-phase-matching concept recently demonstrated during HHG studies in the LPP [38,39] based on the formation of a group of short jets instead of the imperforated extended plasma plume.

IV. THEORY

In the following we present the results of the numerical simulations of two-color MIR-driven HHG in indium ions. We use the three-dimensional time-dependent Schrödinger equation to describe the interaction between the two-color MIR field and the indium ion (atomic units are used throughout, unless otherwise stated):

$$i\frac{\partial \mathbf{\Psi}(\mathbf{r},t)}{\partial t} = \left[-\frac{1}{2}\nabla^2 + \mathbf{V}(\mathbf{r}) - \mathbf{E}(\mathbf{r},t)\cdot\mathbf{r}\right]\mathbf{\Psi}(\mathbf{r},t), \quad (1)$$

where $\mathbf{V}(\mathbf{r})$ is the potential of the plasma system. Here we adopt the model potential introduced in Ref. [21] to reproduce the properties of the indium ion:

$$\mathbf{V}(\mathbf{r}) = -\frac{2}{\sqrt{a^2+\mathbf{r}^2}} + b\exp\left[-\left(\frac{\mathbf{r}-c}{d}\right)^2\right]. \quad (2)$$

This potential can support the metastable state by a potential barrier, which corresponds to the AIS of the ion. The parameters a, b, c, and d are chosen to be 0.65, 1.0, 4.0, and 1.6. There is one dominant transition from the AIS to the ground state ($4d^{10}5s^2\,{}^1S_0 \rightarrow 4d^9 5s^2 5p^1\,P_1$) in the indium ion using this potential [40]. The two-color driving field is synthesized by an x-polarized mid-infrared fundamental field and a y-polarized second-harmonic assistant field. The driving field

is given by

$$\mathbf{E}(\mathbf{r},t) = \begin{cases} E_0 \sin^2(\pi t/T)\cos(\omega_0 t)\mathbf{x} + \sqrt{0.25}E_0 \sin^2(\pi t/T)\cos(2\omega_0 t + \phi)\mathbf{y}, & 0 < t < T, \\ 0, & t > T, \end{cases} \quad (3)$$

where E_0 and ω_0 are the amplitude and central frequency of the 1300 nm laser field. The carrier-envelope phases of the 1300 nm field and the 650 nm field are set as 0. ϕ is the relative phase between the two fields. T is the pulse duration and is given by $T = 10T_0$, where T_0 is the optical cycle of the 1300 nm pulse. The peak intensities of the 1300 nm pulse and the 650 nm pulse are assumed to be 2×10^{14} and 5×10^{13} W cm^{-2}, respectively. Equation (1) can be numerically solved by using the split-operator method [41–43]. Once the evolution of the electron wave function $\Psi(\mathbf{r},t)$ is found, the time-dependent dipole acceleration $a(t)$ can be calculated with the Ehrenfest theorem [44]

$$a(t) = -\langle \Psi(\mathbf{r},t)| \frac{\partial[\mathbf{V}(\mathbf{r}) - \mathbf{E}(\mathbf{r},t)\cdot\mathbf{r}]}{\partial r} |\Psi(\mathbf{r},t)\rangle. \quad (4)$$

The harmonic spectrum $a(\omega)$ is then obtained from the Fourier transform of the dipole acceleration, which is given by

$$a(\omega) = \int_0^T a(t)\exp(-i\omega t)dt. \quad (5)$$

The harmonic spectrum with the two-color MIR field is presented by the red thick curve in Fig. 5. For comparison, the harmonic spectrum with the fundamental field alone is also presented by the blue thin curve. As shown in Fig. 5, the resonant harmonic around 62.2 nm is much more intense than other harmonics. This corresponds to the transition between the ground state and the AIS in the indium ion. Moreover, adding a second harmonic as the assistant field significantly modifies the spectrum. One can clearly see the enhancement of the resonant harmonic yield (the 21st harmonic), the extension of the harmonic cutoff, and the generation of even harmonics (the 20th and 22nd harmonics) in the two-color field compared to the single-color case. Figure 6 presents the two-color harmonic spectra with different wavelengths of the MIR fields. Other laser parameters are the same as those in Fig. 5. It is shown that, when the wavelength of the driving pulses is tuned, different groups of harmonics around the region of the AIS can be selectively enhanced. As the wavelength of the driving pulse varies from 1280 nm to 1380 nm, the tuning of the wavelength of the enhanced radiation is clearly observed, and the resonant harmonic changes from 21st to 22nd order. The theoretical predictions here agree well with the features of two-color resonant HHG observed in experiment as shown in Figs. 3(b) and 3(c).

In Fig. 7(a) we present the variation of intensity of the resonant XUV emission (from $20\omega_0$ to $22\omega_0$) as a function of time in the case of single-color (blue thin curve) and two-color (red thick curve) pumps. Here ω_0 is the frequency of the 1300 nm fundamental pulse. One can see that the XUV radiation is delayed with respect to the laser pulse envelope. Almost all of the resonant harmonics are emitted after five optical cycles. In addition, there are still XUV emissions after the laser pulse has been turned off (from 10 to 20 optical cycles). Such behavior is related to the accumulation of the AIS population in the ion system. Compared to the single-color case, the intensity of the resonant harmonic is significantly

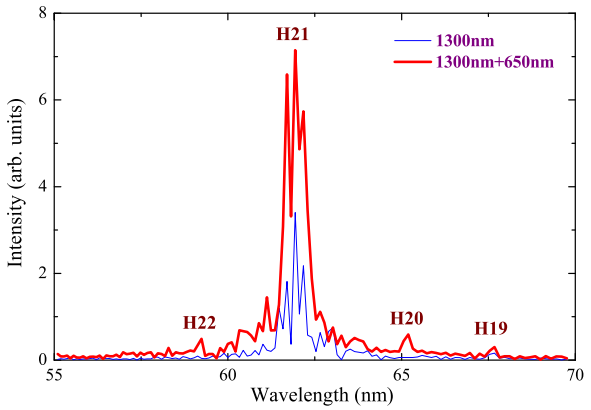

FIG. 5. Simulated harmonic spectra from indium ion with single-color (blue thin line) and two-color (red thick line) fields. The relative phase in the two-color field is 0.

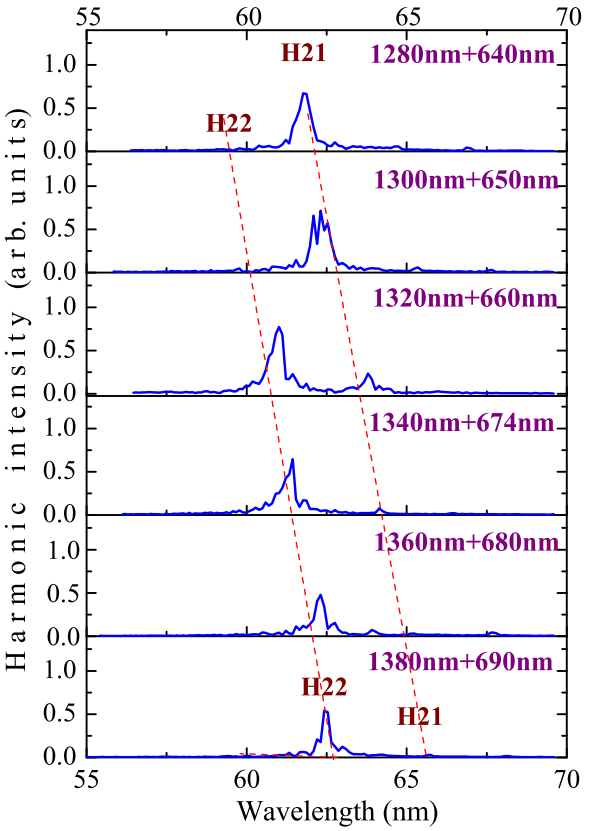

FIG. 6. Simulated variations of high-order harmonic yield using different wavelengths of MIR laser fields. Dashed lines show the tuning of the 21st and 22nd orders of harmonics.

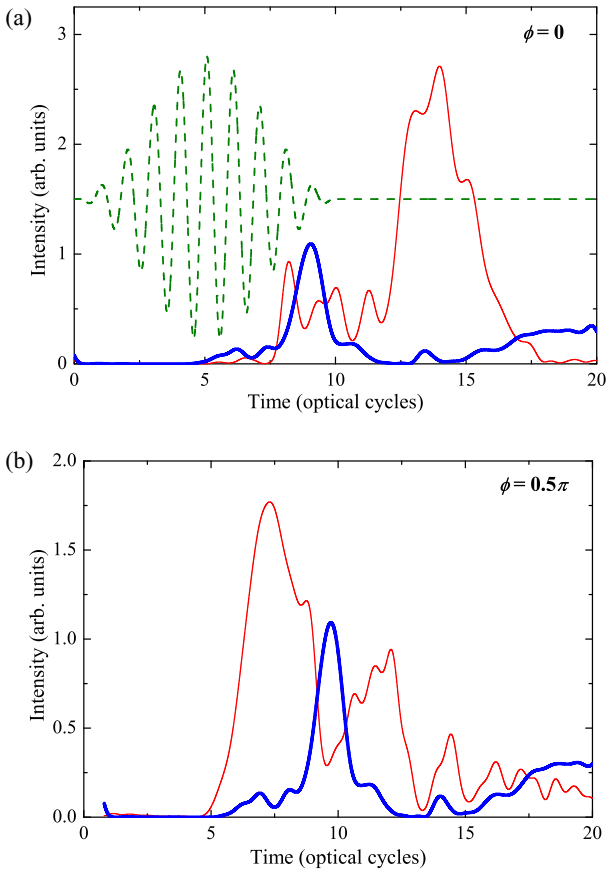

FIG. 7. Temporal profiles of resonant emission (from H20 to H22) in the case of single-color (thick solid blue curve) and two-color (thin solid red curve) pumps. The relative phases in (a) and (b) are 0 and 0.5π, respectively. The dashed green line shows the electric field of the 1300 nm pulse.

increased from 12 to 16 optical cycles in the two-color field. In addition, the harmonic yield in the two-color field shows a more stable distribution around the maximum. In the two-color field, the ionization rate of the ground state is increased by the assistant field. Then more ionized and laser-accelerated electrons can be captured into the AIS. Therefore the transition probability between the AIS and ground state is increased and the intensity of the resonant harmonic is enhanced.

It is worth mentioning that the delay time of the two-color resonant harmonics depends on the parameters of the two-color field. For example, in Fig. 7(a) one can see that the XUV emission in the two-color field is more delayed than that in the single-color case with the relative phase $\phi = 0$. But if we vary ϕ to 0.5π, the maximum emission of the two-color resonant harmonics occurs at about 7.5 optical cycles, while the maximum emission in the single-color field is at about 9 optical cycles [see Fig. 7(b)]. This indicates that the delay effect of the resonant emission in the two-color field is less obvious than that in the single-color field with $\phi = 0.5\pi$. The variation of the temporal profiles of resonant harmonic emission in the two-color field is related to the modulation of autoionization state dynamics by the control field.

We also investigated the influence of the relative phase on the harmonic yield in our scheme. The variations of harmonic

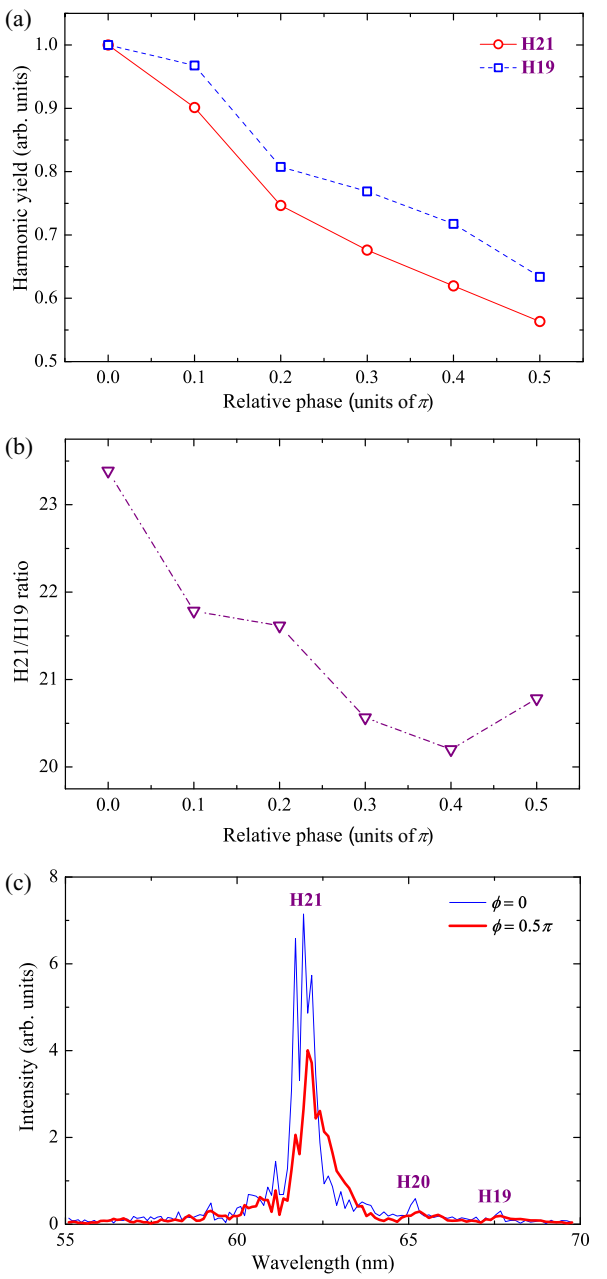

FIG. 8. (a) Dependences of H19 and H21 yields on the relative phase between the 1300 nm and its second-harmonic pulses. (b) Variation of the relative intensities of the 21st and 19th harmonics with relative phase. (c) Simulated harmonic spectra with different relative phases of 0 and 0.5π.

yield for the resonant 21st and nonresonant 19th harmonics are presented by the red solid and blue dashed curves in Fig. 8(a). The yield has been normalized by the case of $\phi = 0.5\pi$ for each curve in order to make a clear comparison. Figure 8(b) shows the variation of the relative intensities of the 21st and 19th harmonics (H21:H19). In Fig. 8(c) we present the comparative harmonic spectra with different relative phases of 0 and 0.5π. One can see that by varying the relative phase of the two-color field one can influence the yield of the resonant and nonresonant harmonics. We found that the change of the harmonic yield in the resonance region is more

significant than that in the nonresonance region. When ϕ varies from 0 to 0.5π, the yield of the 21st harmonic decreases faster than that of the 19th harmonic. Correspondingly the ratio of relative intensities for H21:H19 changes from large values to smaller ones. This indicates that the relative phase of the two-color field may play a role in single-harmonic enhancement during resonance-affected HHG. In addition, we found that the variation of the harmonic spectrum at different ϕ is related to the pulse envelope used in the calculations. When using the trapezoid envelope, the influence of ϕ on the harmonic spectrum is smaller than that using the $\sin^2$ envelope.

V. DISCUSSION

The main message of this work is the demonstration of the use of tunable sources for analysis of the influence of strong resonance on the harmonic efficiency for different orders, in contrast to previous applications of sources with fixed wavelengths, which do not allow the nonlinear spectroscopy of ionic media. The effect of the resonance on the HHG, though not new, is still debated in the literature (see, for example, [45]). Note that no resonance enhancement of harmonics was reported using gaseous media, while harmonic generation in plasmas is a proven road for the analysis of the spectroscopic features of various ionic species using the method of high-order nonlinear spectroscopy. Needless to say, this method allows achieving high fluences of XUV photons. In this paper, we show the difference from previous studies of the influence of resonances on the HHG. In fact, to our knowledge, there are no such studies analyzing this influence, since no tunable laser sources have apparently been applied for the HHG in plasmas, excluding Ref. [46]. Meanwhile, the application of multicycle pulses from OPA for gas harmonics has shown the prospects for generation of attosecond pulses. Thus, the proposed approach could be considered as a road for overcoming the restriction in generation of ultrashort pulses. Plasma harmonics, being proven as an alternative to gas ones, already showed advantages which were not achieved by the latter methods. The use of OPA allowed, as has been shown in this paper, further steps to be achieved in understanding the peculiarities of resonance enhancement.

The application of a two-color pump allowed a significant enhancement of harmonic yield compared with a single-color pump. This claim is not a new one, since it has been proven by many researchers. Here, however, this feature is used for the analysis of resonant HHG in the mid-infrared field, which cannot be realized using a single-color scheme due to the λ^{-5} rule. The use of only a fundamental pump is almost impossible and unpractical for the tasks of this research, since we did not get strong harmonics at all, or they were extremely weak. The use of the second wave is not a trick but rather a necessity to study resonant high-order harmonic generation using a mid-infrared pump.

Moreover, we made changes in the properties of these two pumps and observed the variable response of the medium. One of these changes was the modification of the relative phase between the two pumps. This modification resulted in a significant change in the relative intensities of resonance-enhanced harmonics and other ordinary harmonics [compare the upper and bottom graphs of Fig. 4(b)]. This finding clearly indicates the stronger influence of the relative phase between pumps on the resonance-enhanced harmonics rather than "nonresonant" harmonics. The calculations of the role of the relative phase showed that it was less strong than the experiment shows. The importance of these data is underlined by the fact that they show the relative influence of the phase on the resonance and nonresonant harmonics, since the additional impeding factors (optical losses, imperfect overlap of pulses, etc.) equally influence both harmonics.

The variation of the temporal profiles of resonant emission in the two-color field is related to the modulation of the resonant HHG process by the control field. However, it is very difficult to fully analyze the behavior of the autoionizing state in an exterior laser field (variation of energy, width, decay time, etc.), because this information is entangled in the evolution of the wave function in our current time-dependent Schrödinger (TDSE) model. Our theoretical model (i.e., numerical solution of the 3D TDSE) allowed reproduction of the experimental observations and characterization of the additional spectral and temporal characteristics of the two-color resonant HHG compared to the single-color case. Our results indicate that the dynamics of the autoionization state can be tuned by the two-color field, and therefore the temporal profile of the resonant emission in the two-color field depends on the relative phase.

Since the role of micro- and macroprocesses in resonance enhancement is still debated, this result points out the stronger influence of the former processes. The interpretation of these results probably requires additional studies. Notice that the study [45] also states the same, while analyzing the variations of the coherence length of these harmonics. Thus the analysis of resonance processes by different means may offer different options in definition of the relative influence of the single-particle response and the collective response of the medium on the harmonic yield.

The HHG efficiency in the indium LPP was optimized with respect to various parameters. In particular, the small delay between the 350 ps heating pulses and the 70 fs driving pulses ($<$5 ns) did not allow the observation of harmonics at the used distance between the target and the axis of driving beam propagation. The harmonic generation efficiency abruptly increased once the delay exceeded 5 ns. In the case of indium plasma, the maximal harmonic yield was observed at 35 ns delay. At longer delays, for a fixed distance between the target and the laser beam, the harmonic yield started gradually decreasing until its entire disappearance at $\sim$150 ns. However, we were able to optimize the conversion efficiency at delays larger than 35 ns by increasing the distance between the target and the laser beam. In the present studies, the maximum efficiency of HHG for a 35 ns delay was achieved when the distance between the focal region of the driving beam and the target surface was $\sim$150 μm.

The optimal delay depends on the target material, particularly on its atomic number (Z). We analyzed different targets to reveal the optimal plasma medium at a certain delay between the pulses, corresponding to the maximum conversion of femtosecond radiation into harmonics. It was shown that, at relatively short delays, targets with smaller Z values provide higher conversion efficiency in comparison with heavy targets due to the larger velocities of the former particles. These

measurements were performed at 20 ns delay between the ablated and converted pulses. One might expect this value to be optimal for light ions and atoms because, for heavier ions such as indium ($Z = 49$, atomic weight 115), the time of flight from the target surface to the region of femtosecond radiation propagation exceeds the delay between the pulses because of the lower velocities of In ions in comparison with lighter species.

Below, we briefly discuss the plasma formation above the indium target surface. This process cannot be explained by simple heating of the target surface, its successive melting and evaporation, and the runaway of particles with thermodynamic velocities. These relations are valid for the fairly slow processes induced by long pulses, where the atomic velocity at a target heating temperature of 1000 K is about 7×10^2 m s^{-1}. At these conditions, atoms and ions move by only 15 μm from the target surface during 20 ns. On the assumption that laser plasma formation is determined in our case by such a slow process, the generation of harmonics would be impossible because the radiation to be converted passes at a distance of 150 μm above the target surface. In this case, the particles would reach the interaction region only 200 ns later. At the same time, efficient generation of harmonics (e.g., in indium plasma) started to be observable even at a delay of 20 ns between the pulses and barely occurs at delays above 150 ns. This also holds true for formation of other plasmas.

This inconsistency between the thermal model of propagation of evaporated material and the observed efficient HHG in LPP at small delays between the ablating and driving pulses is explained within another model of plasma formation, specifically, plasma explosion during target ablation by short pulses. The dynamics of plasma front propagation during laser ablation by short pulses has been analyzed in a number of studies (see, e.g., [47,48] and references therein). A numerical analysis of plasma formation from a target irradiated with a single laser pulse was reported in the monograph [47]. The velocities of the plasma front in accordance with the plasma explosion model were in the range of 1×10^4 to 1×10^5 m s^{-1}.

In experiments, the dynamics of plasma origin and propagation can be analyzed using the shadowgraph technique. The spatial characteristics of the laser plasma formed by short pulses under similar conditions on the surfaces of lighter (boron, $Z = 5$) and heavier (manganese, $Z = 25$) targets were reported in Ref. [49]. In the case of the heavier target (Mn), the plasma front propagated at a velocity of 6×10^4 m s^{-1}. The plasma front passed through a distance of 130 μm after a few nanoseconds, rather than several hundreds of nanoseconds, in accordance with the above-described thermal model of plasma expansion. One can assume that, in the case of In ions possessing a twice heavier mass than Mn, the slower movement causes a later appearance of the plasma cloud in the area of laser beam propagation. Obviously, the formation of the optimal plasma is not limited by the occurrence of the plasma front in the propagation region of radiation to be converted. To this end, some time is necessary for the concentration of particles responsible for harmonic generation to reach a certain value.

The application of fundamental waves together with an assistant field dramatically changes the efficiency of HHG and allows the observation of the resonantly enhanced harmonic along with the enhanced nearby harmonics. The influence of the assistant (H2) field on HHG did not crucially depend on the relative intensities of the two pumps. In the present studies, the maximal efficiency of second-harmonic generation using the 1310 nm pulses (27%) means the ratio of the second-harmonic pulse energy and the whole 1310 nm pulse energy (measured before the propagation of the BBO). This efficiency shows that the ratio of assistant (655 nm) and driving (1310 nm) pulse energies inside the plasma was approximately 1:3. The theoretical calculations took into account different ratios of the two interacting pulses. The variation of this ratio between 1:5 and 1:3 did not change definitely the conclusions defined from the calculations of the theoretical model used. In the present studies, we showed calculations of harmonic spectra using the 1:4 ratio. The role of the second field in the ratio of pulse energies used was similar to the influence of this assistant field at rather smaller ratios. In particular, in the case of using the 1:5 and 1:20 ratios, similar strong enhancement of the odd harmonics as well as equal odd and even harmonic intensities were achieved in the previous studies using the 800-nm-class lasers [50,51].

As was already mentioned, the first observation of resonant HHG was reported in Ref. [14] for a low-charged indium plasma prepared by laser ablation. In those and other experiments with indium plasma [40,52–54], the 13th harmonic of 800 nm laser radiation was a few tens of times more intense than neighboring harmonics. This phenomenon is attributed to a strong multiphoton resonance with exceptionally strong transition of the single-charged indium ion, which can easily be Stark shifted toward the 13th harmonic of the 800 nm pump radiation.

The enhancement of the 13th harmonic emission from the indium plasma observed in those and present studies is due to the influence of radiative transitions between the $4d^{10}5s^2\,{}^1S_0$ ground state of In II and the low-lying $4d^9 5s^2 np$ transition array of In II. Among them, the transition at 19.92 eV (62.24 nm) corresponding to the $4d^{10}5s^2\,{}^1S_0 \rightarrow 4d^9 5s^2 5p\,{}^1P_1$ transition of In II is exceptionally strong. The gf value, the product of the oscillator strength f of a transition and the statistical weight g of the lower level, of this transition has been calculated to be $gf = 1.11$ [55], which is more than 12 times larger than that of any other transition from the ground state of In II. This transition is energetically close to the 13th harmonic ($h\nu_{13\mathrm{H}} = 20.15$ eV or $\lambda = 61.53$ nm) of 800 nm radiation and the 21st harmonic ($h\nu_{21\mathrm{H}} = 20.02$ eV or $\lambda = 61.9$ nm) of 1300 nm radiation, thereby resonantly enhancing its intensity.

VI. CONCLUSIONS

In conclusion, the main scientific interest of this research was about using the tunable pump to get a better understanding of the HHG at resonances. To demonstrate this we have shown many individual spectra at different wavelengths of the fundamental pump. The tunability was practically unlimited since the tuning of the fundamental wavelength allowed shifting the wavelength of the high-order harmonic over the wavelength of the neighboring harmonic, which means the overlap of a full octave. We have shown that tuning of odd and even high-order harmonics along the strong resonance of laser-produced indium plasma using the optical parametric amplifier of white-light continuum radiation (1250–1400 nm) allows the observation of different harmonics enhanced in the

vicinity of the strong AIS of In II ions. We have demonstrated various peculiarities and discussed the theoretical model of the phenomenon of tunable harmonics enhancement in the region of 62 nm using indium plasma. We increased the intensity of the harmonics generated by such a long fundamental wavelength using a two-color laser field with the second harmonic wave orthogonally polarized to the fundamental one. The selective enhancement of the resonant harmonics in the two-color scheme has been confirmed by a theoretical model. Our approach allowed us to precisely analyze the role of the AIS of In ions by tuning various harmonics through the resonance under consideration. These studies show that the application of tunable MIR pulses can be used to optimize the earlier reported resonance enhancement of specific harmonics as well as to identify additional areas of harmonic enhancement.

[1] P. B. Corkum and F. Krausz, Nat. Phys. **3**, 381 (2007).
[2] J. P. Marangos, S. Baker, N. Kajumba, J. S. Robinson, J. W. G. Tisch, and R. Torres, Phys. Chem. Chem. Phys. **10**, 35 (2008).
[3] C. Jin, H. J. Wörner, V. Tosa, A.-T. Le, J. B. Bertrand, R. R. Lucchese, P. B. Corkum, D. M. Villeneuve, and C. D. Lin, J. Phys. B: At. Mol. Opt. Phys. **44**, 095601 (2011).
[4] K. J. Schafer, B. Yang, L. F. DiMauro, and K. C. Kulander, Phys. Rev. Lett. **70**, 1599 (1993).
[5] P. B. Corkum, Phys. Rev. Lett. **71**, 1994 (1993).
[6] J. Levesque, D. Zeidler, J. P. Marangos, P. B. Corkum, and D. M. Villeneuve, Phys. Rev. Lett. **98**, 183903 (2007).
[7] R. A. Ganeev, H. Singhal, P. A. Naik, V. Arora, U. Chakravarty, J. A. Chakera, R. A. Khan, P. V. Redkin, M. Raghuramaiah, and P. D. Gupta, J. Opt. Soc. Am. B **23**, 2535 (2006).
[8] M. Suzuki, M. Baba, H. Kuroda, R. A. Ganeev, and T. Ozaki, Opt. Express **15**, 1161 (2007).
[9] D. Shiner, B. E. Schmidt, C. Trallero-Herrero, H. J. Wörner, S. Patchkovskii, P. B. Corkum, J.-C. Kieffer, F. Légaré, and D. M. Villeneuve, Nat. Phys. **7**, 464 (2011).
[10] U. Fano, Phys. Rev. **124**, 1866 (1961).
[11] F. Keller and H. Lefebvre-Brion, Z. Phys. D: At. Mol. Clusters **4**, 15 (1986).
[12] M. Y. Amusia and J.-P. Connerade, Rep. Prog. Phys. **63**, 41 (2000).
[13] J. F. Reintjes, *Nonlinear Optical Parametric Processes in Liquids and Gases* (Academic Press, Orlando, 1984).
[14] R. A. Ganeev, M. Suzuki, T. Ozaki, M. Baba, and H. Kuroda, Opt. Lett. **31**, 1699 (2006).
[15] E. S. Toma, P. Antoine, A. de Bohan, and H. G. Muller, J. Phys. B: At. Mol. Opt. Phys. **32**, 5843 (1999).
[16] M. B. Gaarde and K. J. Schafer, Phys. Rev. A **64**, 013820 (2001).
[17] R. Bartels, S. Backus, E. Zeek, L. Misoguti, G. Vdovin, I. P. Christov, M. M. Murnane, and H. C. Kapteyn, Nature (London) **406**, 164 (2000).
[18] R. Taïeb, V. Véniard, J. Wassaf, and A. Maquet, Phys. Rev. A **68**, 033403 (2003).
[19] D. B. Milošević, J. Phys. B: At. Mol. Opt. Phys. **40**, 3367 (2007).
[20] D. B. Milošević, Phys. Rev. A **81**, 023802 (2010).
[21] V. Strelkov, Phys. Rev. Lett. **104**, 123901 (2010).
[22] M. V. Frolov, N. L. Manakov, and A. F. Starace, Phys. Rev. A **82**, 023424 (2010).
[23] P. V. Redkin and R. A. Ganeev, Phys. Rev. A **81**, 063825 (2010).
[24] M. Tudorovskaya and M. Lein, Phys. Rev. A **84**, 013430 (2011).
[25] Pengfei Lan, E. J. Takahashi, and K. Midorikawa, Phys. Rev. A **81**, 061802 (2010).
[26] E. Cormier and M. Lewenstein, Eur. Phys. J. D **12**, 227 (2000).
[27] I. J. Kim, C. M. Kim, H. T. Kim, G. H. Lee, Y. S. Lee, J. Y. Park, D. J. Cho, and C. H. Nam, Phys. Rev. Lett. **94**, 243901 (2005).
[28] J. Mauritsson, P. Johnsson, E. Gustafsson, A. L'Huillier, K. J. Schafer, and M. B. Gaarde, Phys. Rev. Lett. **97**, 013001 (2006).
[29] T. Pfeifer, L. Gallmann, M. J. Abel, D. M. Neumark, and S. R. Leone, Opt. Lett. **31**, 975 (2006).
[30] Y. Yu, X. Song, Y. Fu, R. Li, Y. Cheng, and Z. Xu, Opt. Express **16**, 686 (2008).
[31] X.-S. Liu and N.-N. Li, J. Phys. B: At. Mol. Opt. Phys. **41**, 015602 (2008).
[32] D. Charalambidis, P. Tzallas, E. P. Benis, E. Skantzakis, G. Maravelias, L. A. A. Nikolopoulos, A. P. Conde, and G. D. Tsakiris, New J. Phys. **10**, 025018 (2008).
[33] I. J. Kim, G. H. Lee, S. B. Park, Y. S. Lee, T. K. Kim, C. H. Nam, T. Mocek, and K. Jakubczak, Appl. Phys. Lett. **92**, 021125 (2008).
[34] L. Brugnera, D. J. Hoffmann, T. Siegel, F. Frank, A. Zair, J. W. G. Tisch, and J. P. Marangos, Phys. Rev. Lett. **107**, 153902 (2011).
[35] H. R. Telle, G. Steinmeyer, A. E.Dunlop, J. Stenger, D.H. Sutter, and U. Keller, Appl. Phys. B **69**, 327 (1999).
[36] V. Tosa, E. Takahashi, Y. Nabekawa, and K. Midorikawa, Phys. Rev. A **67**, 063817 (2003).
[37] H. R. Lange, A. Chiron, J. F. Ripoche, A. Mysyrowicz, P. Breger, and P. Agostini, Phys. Rev. Lett. **81**, 1611 (1998).
[38] R. A. Ganeev, M. Suzuki, and H. Kuroda, Phys. Rev. A **89**, 033821 (2014).
[39] R. A. Ganeev, V. Tosa, K. Kovács, M. Suzuki, S. Yoneya, and H. Kuroda, Phys. Rev. A **91**, 043823 (2015).
[40] R. A. Ganeev, T. Witting, C. Hutchison, V. V. Strelkov, F. Frank, M. Castillejo, I. Lopez-Quintas, Z. Abdelrahman, J. W. G. Tisch, and J. P. Marangos, Phys. Rev. A **88**, 033838 (2013).
[41] J. L. Krause, K. J. Schafer, and K. C. Kulander, Phys. Rev. A **45**, 4998 (1992).
[42] M. Protopapas, C. H. Keitel, and P. L. Knight, Rep. Prog. Phys. **60**, 389 (1997).
[43] A. Castro, H. Appel, M. Oliveira, C. A. Rozzi, X. Andrade, F. Lorenzen, M. A. L. Marques, E. K. U. Gross, and A. Rubio, Phys. Status Solidi B **243**, 2465 (2006).
[44] K. Burnett, V. C. Reed, J. Cooper, and P. L. Knight, Phys. Rev. A **45**, 3347 (1992).
[45] N. Rosenthal and G. Marcus, Phys. Rev. Lett. **115**, 133901 (2015).
[46] C. Hutchison, R. A. Ganeev, M. Castillejo, I. Lopez-Quintas, A. Zair, S. J. Weber, F. McGrath, Z. Abdelrahman, M. Oppermann,

M. Martín, D. Y. Lei, S. A. Maier, J. W. Tisch, and J. P. Marangos, Phys. Chem. Chem. Phys. **15**, 12308 (2013).

[47] H. Hora, *Plasmas at High Temperature and Density* (Springer, Heidelberg, 1991).

[48] B. Rus, P. Zeitoun, T. Mosek, S. Sebban, M. Kálal, A. Demir, G. Jamelot, A. Klisnick, B. Králiková, J. Skála, and G. J. Tallents, Phys. Rev. A **56**, 4229 (1997).

[49] R. A. Ganeev, M. Suzuki, M. Baba, and H. Kuroda, Opt. Spectrosc. **99**, 1000 (2005).

[50] R. A. Ganeev, H. Singhal, P. A. Naik, J. A. Chakera, H. S. Vora, R. A. Khan, and P. D. Gupta, Phys. Rev. A **82**, 053831 (2010).

[51] R. A. Ganeev, C. Hutchison, A. Zaïr, T. Witting, F. Frank, W. A. Okell, J. W. G. Tisch, and J. P. Marangos, Opt. Express **20**, 90 (2012).

[52] R. A. Ganeev, H. Singhal, P. A. Naik, V. Arora, U. Chakravarty, J. A. Chakera, R. A. Khan, I. A. Kulagin, P. V. Redkin, M. Raghuramaiah, and P. D. Gupta, Phys. Rev. A **74**, 063824 (2006).

[53] R. A. Ganeev, L. B. Elouga Bom, J.-C. Kieffer, and T. Ozaki, Phys. Rev. A **75**, 063806 (2007).

[54] R. A. Ganeev, J. Zheng, M. Wöstmann, H. Witte, P. V. Redkin, and H. Zacharias, Eur. Phys. J. D **68**, 325 (2014).

[55] G. Duffy and P. Dunne, J. Phys. B **34**, L173 (2001).